Journal of
Water & Climate Change

IWA PUBLISHING

Journal of Water and Climate Change Vol 15 No 3, 1282 doi: 10.2166/wcc.2024.577

Climate variability, trend, and associated risks: Tana sub-basin, Ethiopia

Bewuketu Abebe Tesfaw [a,b,*], Bloodless Dzwairo [b,c] and Dejene Sahlu [d]

[a] Abbay Basin Administration Office, Bahir Dar, Ethiopia
[b] Department of Civil Engineering, Durban University of Technology, Midlands, P.O. Box 101112, Imbali 3209, South Africa
[c] Durban University of Technology, Institute for Water and Wastewater Technology, P.O. Box 1334, Durban 4001, South Africa
[d] Bahir Dar University, Bahir Dar, Ethiopia
*Corresponding author. E-mail: bewuketu.at@gmail.com; 22063693@dut4life.ac.za

BAT, 0000-0001-7341-9089; BD, 0000-0002-0127-2978; DS, 0000-0001-7253-9150

ABSTRACT

The study focused on analyzing the variability and trends of climate parameters in the Tana sub-basin. Various statistical methods and indices were employed to assess precipitation and temperature patterns in the region. The findings indicated a statistically non-significant increasing trend in rainfall across the sub-basin, with values ranging from 1.64 to 5.37 mm/year. In terms of temperature, there was an increasing trend observed, but it was also not statistically significant. The seasonality index ranged between 0.87 and 1.03, indicating different rainfall distribution patterns. In 36.69% of the sub-basin, rainfall occurs in marked seasonal patterns with a long dry season, and the remaining (63.31%) is concentrated in 3 or fewer months, indicating a different rainfall distribution pattern. In addition, the study assessed the precipitation concentration and found that 57.5% of the rainfall data exhibited a strong irregular concentration, 41.5% showed an irregular concentration, and 1% exhibited a moderate concentration. The study underscores the presence of climate variability and trends in the Tana sub-basin, emphasizing the need to align agricultural and water resource management practices with the observed climate variability.

Key words: climate variability, rainfall, Tana sub-basin, temperature, trend

HIGHLIGHTS

- The study quantifies the magnitude of climate variability and trend of the study area.
- The study has accredited contributions to climate variability, trends, and associated risks.
- It provides perceptible conclusions that could assist stakeholders and decision-makers in making prominent choices regarding natural resource planning and management.
- The result will be used as a guideline for further studies on related issues in the area.

GRAPHICAL ABSTRACT

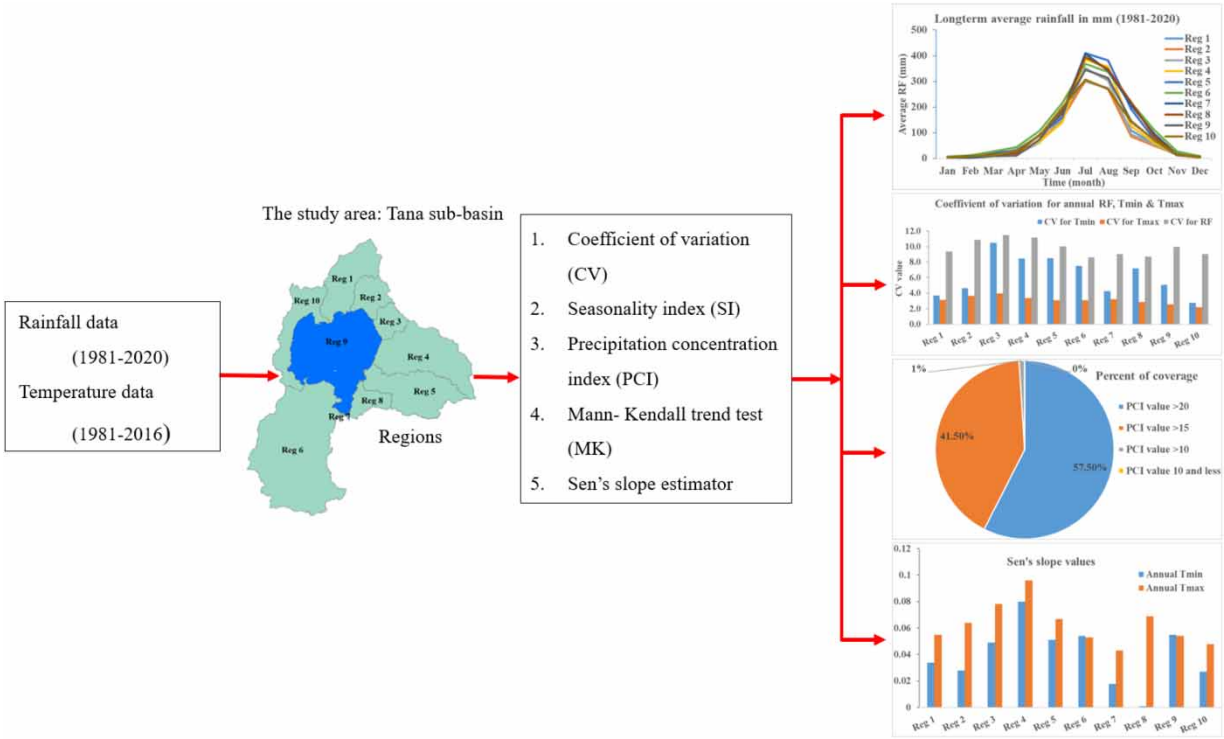

1. INTRODUCTION

Climate change is mainly referred to as the long-term fluctuations in weather parameters of a large area with statistical significance (Getachew & Manjunatha 2021). Climate change is one of the world's major challenges in the 21st century (Field 2014; Abidoye & Odusola 2015; Reidmiller *et al.* 2018), and its adverse impacts challenge people's socioeconomic activities, livelihood, health, and food security (Clarke *et al.* 2012). Global warming and climate variability are the emerging foremost environmental problems and global threats in the 21st century, particularly in developing countries (Birara *et al.* 2018; Habte *et al.* 2021). Climate variability and change, its impacts, and the associated vulnerabilities, are rising environmental issues worldwide (Makenzi *et al.* 2013). The fifth assessment report of the IPCC (IPCC 2013) indicated that the global mean temperature showed a warming trend of 0.85 °C (0.65–1.06) over the period 1880–2012. Already, most regional studies use long-term changes in temperature and rainfall patterns as a proxy indicator of climate change (Enyew 2014; Addisu *et al.* 2015; Birara *et al.* 2018, 2020; Berihun *et al.* 2019; Esayas *et al.* 2019; Tenagashaw & Andualem 2022). Many of the developing countries, mainly those found in sub-Saharan Africa, are significantly influenced by the global average temperature rise and its consequences (IPCC 2012). The studies by Belay *et al.* (2021) and Getachew & Manjunatha (2021) indicated that Earth's climate change and variability are the results of either natural variability or anthropogenic (human) activity, in combination. The anthropogenic causes arise from various activities such as excessive usage of fossil fuels, deforestation, and changes in agricultural practices are believed to increase the atmospheric concentration of greenhouse gases and temperature (UNFCCC 2007; Saroar & Filho 2016), and could alter the natural atmospheric processes for many decades (Hassan *et al.* 2014), while the natural causes include changes in solar activities, orbital parameters, and volcanic eruptions. Anthropogenic (human) activity has changed the earth's environment over the past century, while more changes are expected in the coming few decades, even if strong mitigation measures are taken (IPCC 2013).

The countries located in the sub-Sahara region include Ethiopia, whose economy is significantly affected by climate variability (Birara *et al.* 2018). The Blue Nile River Basin is one of the region's most sensitive basins to changing climate and water resource variability (Kim & Kaluarachchi 2009). Various studies have investigated historical trends of climate change and variability in Ethiopia. For instance, a 0.37 °C per decade increase was observed in minimum temperature between 1951 and 2006 by McSweeney *et al.* (2008), whereas, a 0.2–0.28 °C rise per decade in the average annual maximum temperature

between 1960 and 2006 was observed by Keller (2009) and Eshetu *et al.* (2014). El Niño/Southern Oscillation has a significant influence on rainfall over Eastern Africa, especially during the October–December rainfall season (Awange *et al.* 2014; Omondi *et al.* 2014). The studies by Abera *et al.* (2020) indicated that high rainfall variability in Ethiopia is observed especially in the area where agricultural-dependent rural people are densely populated (highland regions). The study area is one of the areas in Ethiopia influenced by population pressure dominantly dependent on agriculture (Abera *et al.* 2020) and high expansion of cultivation practices (Tesfaw *et al.* 2023). A rapidly growing and dense population in the area is putting unprecedented pressure on natural resources. The annual and seasonal variability of rainfall significantly affected agricultural productivity, pastoralists, and animals in Ethiopia (Seleshi & Zanke 2004; Makenzi *et al.* 2013). Lake Tana is a lake in the Tana sub-basin, which is highly sensitive to variations in rainfall as well as variations in river inflows and evaporation (Kebede *et al.* 2006). Setegn *et al.* (2009) showed that inflow river discharge to Lake Tana contributes over 90% of the lake inflow. It is, thus, very likely that changes in river inflow would also change the volume of the lake and the water balance, which could ultimately adversely impact the lake ecosystem. Analyzing the spatial-temporal distribution of rainfall and detecting trends is the key to healthy ecosystem functions and sustaining agricultural production (Krishan *et al.* 2012; Meshesha *et al.* 2018; Worku *et al.* 2018). Therefore, this study was initiated to analyze climate variability, trends, and associated risks of the climate parameters (temperature and rainfall) in the Tana sub-basin, Ethiopia. The seasonal and annual variability of rainfall and temperature were assessed, and the concentration of precipitation was computed. The findings of this study will provide valuable information for planners and decision-makers in the region. Understanding the variability and trends of temperature and rainfall is crucial for developing appropriate adaptation and mitigation strategies to address the potential risks associated with climate change. This information can also be used to inform agricultural practices, water resource management, and infrastructure development in the Tana sub-basin. Overall, this study will contribute to a better understanding of the climate dynamics in the Tana sub-basin and provide valuable insights for sustainable development and climate resilience in the region.

2. MATERIALS AND METHODS

2.1. Study area

Tana sub-basin is located between 36°45′ to 38°15′ East and 10°57′ to 12°46′ North. The study area covers 15,070.14 km^2, with 20% of this area being Lake Tana (Tesfaw *et al.* 2023). The average elevation of the study area is about 2,026.54 MASL. The highest elevation of the sub-basin exit is in the eastern part with an elevation of 4,112 MASL and the lowest is in the southeast part near Bahir Dar town in the Amhara region with an elevation of 1,777 MASL. The drainage area of the sub-basin is composed of numerous rivers and streams (Kebede *et al.* 2006). The sub-basin is divided into 10 watersheds (regions) in this study, and Dek Estifanos is bounded by Lake Tana (Reg 9 in Figure 1), and is considered a part of the lake for this study.

According to the annual rainfall characteristics of Ethiopia, there are three rainy seasons (Gissila *et al.* 2004; Segele & Lamb 2005; Korecha & Barnston 2007; Haile *et al.* 2009). The country's main rainy season is from June to September, the dry season from October to January, and the small rainy season from February to May. Unimodal rainfall distribution occurs in the study area (Getachew & Manjunatha 2021), while its mean annual rainfall is estimated to be 1,280 mm (Setegn *et al.* 2008; Birara *et al.* 2018). Most rainfall falls during the major rainfall season from June to September (Alemu *et al.* 2020). The mean annual temperature of the study area is 21 °C by Weldegerima *et al.* (2018). The annual actual evapotranspiration of the sub-basin was 1,036 mm by Allam *et al.* (2016) and 733 mm by Setegn *et al.* (2008).

2.2. Data collection

The climatic variables used for the study, including rainfall (1981–2020) and maximum and minimum temperature (1981–2016), were obtained from the Enhancing National Climate Services (ENACTS) products provided by the National Meteorological Agency (NMA). The ENACTS products (https://iri.columbia.edu/resources/enacts/) used in this study were derived from a grid and blended dataset, which combined ground observation station data with satellite estimates for rainfall, digital elevation models, and reanalysis products for temperature (Dinku *et al.* 2017).

The process involved applying the average weight method to generate time series climate data from the ENACTS grid product for the ten regions of the study area. The quality of the data was ensured by checking it against ground observation station data. In addition, the ENACTS dataset, along with nearby observed data, underwent performance evaluation using criteria such as Nash–Sutcliffe efficiency, coefficient of determination (R^2), and Percent Bias. This comprehensive approach

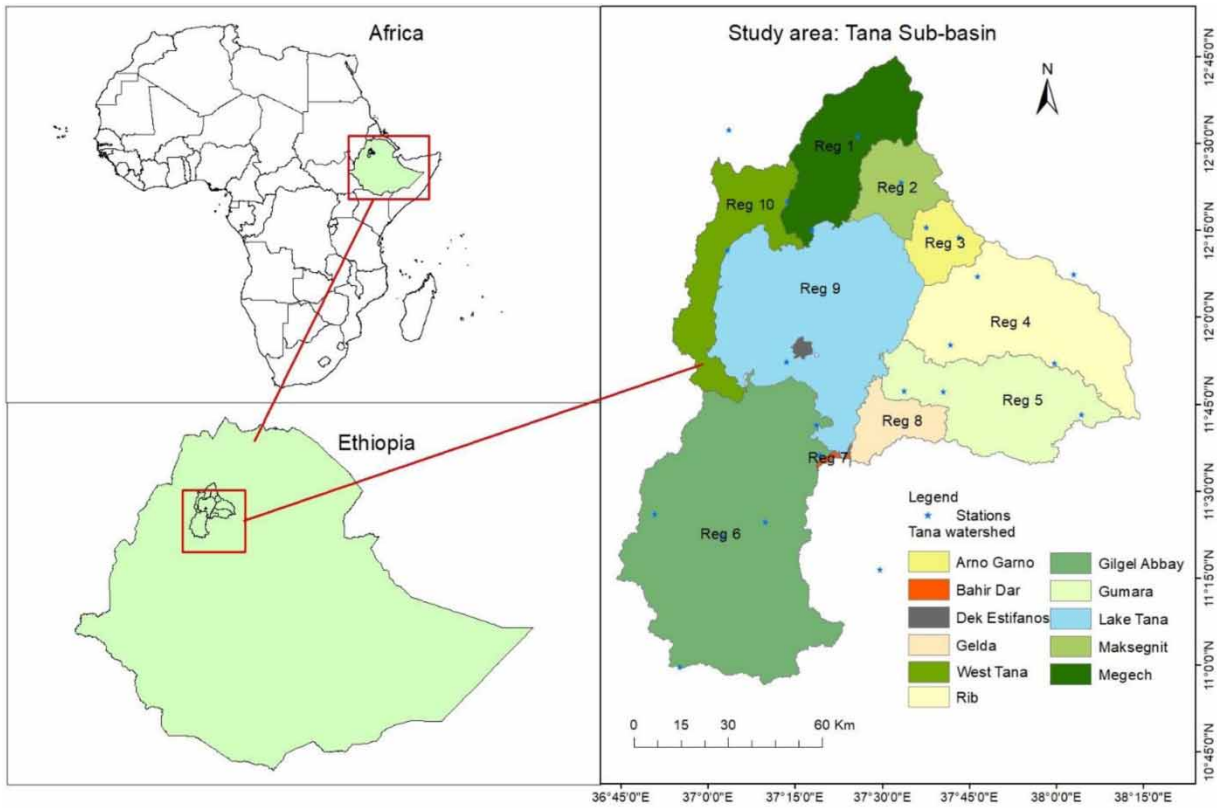

Figure 1 | The location of the study area: Tana sub-basin.

to data collection and validation ensures that the study is based on high-quality and reliable climate data, which is essential for accurate and meaningful analysis.

2.3. Data analysis

The coefficient of variation (CV), seasonality index (SI), precipitation concentration index (PCI), Mann–Kendall (MK) trend test, and Sen's slope estimator were used to determine the variability, trend, duration, and magnitude of annual, seasonal, and monthly precipitation and temperature in the study area (Verma *et al.* 2022; Kumar *et al.* 2023). Monthly rainfall and temperature data were used. Monthly rainfall and temperature data were used covering the period 1981–2020 and 1981–2016, respectively, as an input.

2.3.1. Coefficient of variation

The CV was computed to evaluate the annual, seasonal, and monthly variability of rainfall, and minimum and maximum temperature across the study area during the recording period. The degree of rainfall and temperature variability is classified into three classes, namely, high (CV > 30%), moderate (20% < CV < 30%), and low (CV < 20%) (NMSA 1996; Hare 2003). The value of CV can be computed using Equation (1)

$$\mathrm{CV} = \frac{\sigma}{\bar{x}} \times 100 \tag{1}$$

where CV is the coefficient of variation, σ is the standard deviation, and $\bar{x}$ is the mean precipitation and temperature of the recording period.

2.3.2. Rainfall regime classifications

The rainfall regime can be classified using the value of the SI (Walsh & Lawler 1981). The SI expressed the standardized timing and duration of rainfall without the influence of magnitude. The most common method adopted to compute the SI

of the stations to define the rainfall regimes was proposed by Walsh & Lawler (1981). These indices can show the differences in relative seasonality even in areas with two or three rainfall peaks throughout the year. The SI is defined as the sum of the absolute deviation of mean monthly rainfall from the overall monthly mean and divided by the mean annual rainfall.

$$\mathrm{SI} = \frac{1}{R}\sum_{n=1}^{n=12} \mathrm{abs}\left(X_n - \frac{R}{12}\right) \tag{2}$$

The value of the SI varies from 0 (when all months share the same amount of rainfall) to 1.83 (when all rainfall incidences occur in a single month). Walsh & Lawler (1981) also proposed rainfall regime classification based on SI values (Table 1). The classification is further redefined based on the rainfall duration during the year (Table 1).

2.3.3. Precipitation concentration index

The PCI was used to evaluate the annual, seasonal, and monthly distribution of the rainfall in the study area: Tana sub-basin. It is also used to indicate the hydrological risks of floods and drought occasions (De Luís *et al.* 2000; Gocic & Trajkovic 2013) and can be calculated using Equation (3):

$$\mathrm{PCI} = \frac{\sum_{i=1}^{12} \mathrm{Pi}^2}{\left(\sum_{i=1}^{12} \mathrm{Pi}\right)^2} \tag{3}$$

where Pi is the precipitation amount of *i*th month

The value of PCI less than 10 indicates the uniform distribution of precipitation; values between 11 and 15 represent moderate precipitation concentration; values between 16 and 20 indicate the irregular distribution of precipitation and the value which is above 20 unit shows a strong irregular precipitation distribution across the area (Oliver 1980; Belay *et al.* 2021; Edo *et al.* 2021).

2.3.4. MK trend test

The MK trend test is one of the most well-known and widely used methods to detect climate trends in time series data (Addisu *et al.* 2015; Asfaw *et al.* 2018). The details of the MK test are provided in the studies by Mann (1945) and Kendall (1975). It is used to detect monotonically (increasing or decreasing) trends on seasonal and annual basis of climate parameters. The MK trend test and Sen's estimator were employed to investigate the existence of long-term change for both rainfall and temperature indices. Seasonal and annual trend change detection with the MK test is less affected by climate outliers (Sen 1968; Birsan *et al.* 2005). Two types of statistics depend upon the number of data values i.e., S is the statistics used if several data values are less than 10 while Z is the statistics (normal approximation/distribution) for data values greater than or equal to 10. S is calculated based on total signs (it is always between -1, 0, and 1). In cases in which $N > 10$, the standard Z is calculated as follows:

$$S = \sum_{i=1}^{n-1}\sum_{j=i+1}^{n} \mathrm{sgn}(Xj - Xi) \tag{4}$$

where the Xi is the actual time data for the time series of $i = 1, 2, 3, \ldots, n$, and n is the sample size.

Table 1 | Redefined classification of the SI based on rainfall duration

Class code	Rainfall regime	SI	Rainfall duration in day
1	Very equable	≤0.19	≥270
2	Equable with a definite wetter season	0.20–0.39	180–269
3	Rather seasonal with a short drier season	0.40–0.59	150–179
4	Seasonal	0.60–0.79	120–149
5	Markedly seasonal with a long drier season	0.80–0.99	90–119
6	Most rain in 3 or less month	1.00–1.19	60–89
7	Extreme, almost all rain in 1–2 months	≥1.20	<60

The value of sgn (Xj – Xi) is calculated as follows:

$$\begin{aligned}\text{sgn}(\text{Xj}-\text{Xi}) &= 1 \quad \text{if Xj}-\text{Xi}>0\\ &= 0 \quad \text{if Xj}-\text{Xi}=0\\ &= -1 \quad \text{if Xj}-\text{Xi}<0\end{aligned} \tag{5}$$

The *S*-statistics approximately behave as normally distributed, and the test is performed with normal distribution with the mean and variation as given in the below equations:

$$\begin{aligned}&E(S)=0\\ &\text{and}\\ &\text{Var}(S)=\frac{n(n-1)(2n+5)-\sum_{i=1}^{m} t(t-1)(2t+5)}{18}.\end{aligned} \tag{6}$$

Standard *Z* for one limit test is as shown below in Equation (7): the positive value of *Z* shows an increasing trend and the negative value shows a decreasing trend.

$$Z=\begin{cases}(s-1)/(\sqrt{\text{Var}(s)}, & s>0\\ 0, & S=0\\ \dfrac{s+1}{\sqrt{\text{Var}\,(s)}}, & s<0\end{cases} \tag{7}$$

Then, the MK test from the *Z* value was computed based on monthly, seasonal, and annual rainfall time series data.

2.3.5. Sen's slope estimator

In addition to trend identification, the magnitude of the drift (gradual increase or decrease) was also computed using Sen's slope (β) method (Kassie *et al.* 2014; Belay *et al.* 2021). This is a nonparametric method with which the slope of *N* pairs of data points is estimated.

$$\beta=\left(\frac{\text{xj}-\text{xi}}{j-i}\right) \tag{8}$$

where β represents the median value of the slope values between data measurements xi and xj at the time steps *i* and *j* ($i<j$), respectively. A positive value of Sen's slope (β) indicates an increasing trend and a negative value suggests a decreasing trend in the time series. The trend from Sen's slope (β) estimation was computed based on monthly, seasonal, and annual rainfall and temperature time series data.

3. RESULTS AND DISCUSSION

3.1. Climatic variability

Annually, the value of the CV was less than 20% which indicated that the study area in all regions had a lower variability of rainfall and temperature during 1981–2020 and 1981–2016, respectively (Figures 2–5). Across the regions, the north, northeast, central, and eastern parts of the study area show high annual rainfall variability while the south and eastern part of the sub-basin show relatively high annual minimum temperature variability. In the north, northeast, east, and southern parts of the study area, results show relatively high annual maximum temperature variability.

The temporal variation of monthly rainfall was high compared to the temporal variation of monthly temperature in the study area, as indicated in Figures 2, 4, and 5. The significant variability of monthly rainfall across the region emphasizes the dynamic nature of precipitation patterns in the study area. This variability likely has important implications for various sectors, including agriculture, water resource management, and ecosystem dynamics (Wubneh *et al.* 2023). High rainfall variability (CV > 30) was observed from February to May, October to December, and in January for some parts of the regions

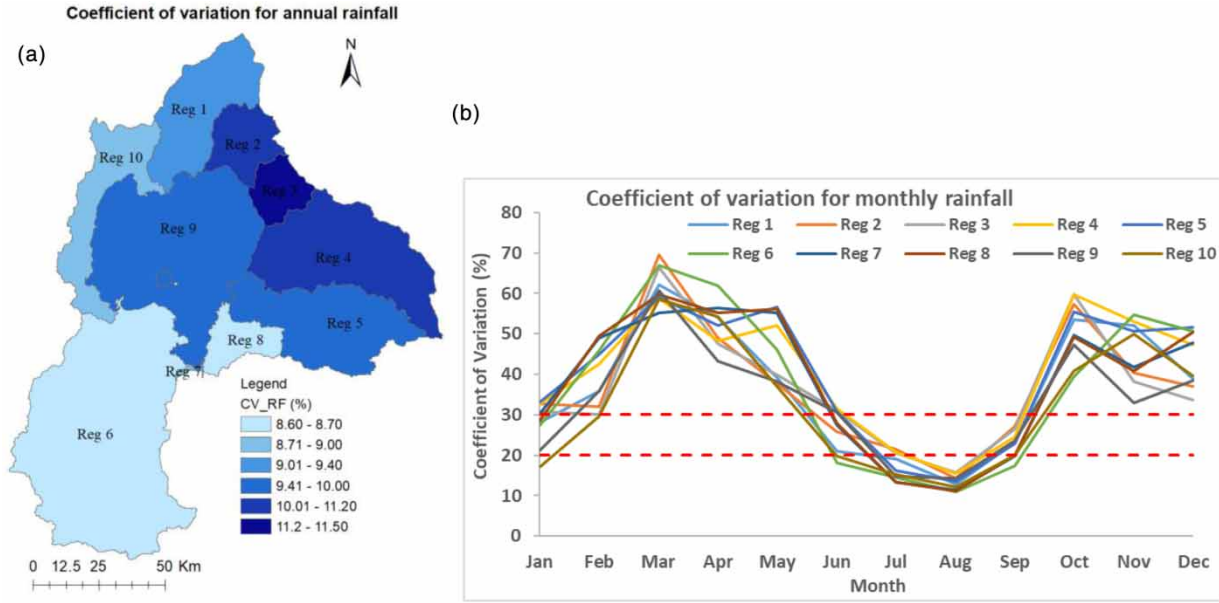

Figure 2 | CV for (a) annual and (b) monthly rainfall across the regions.

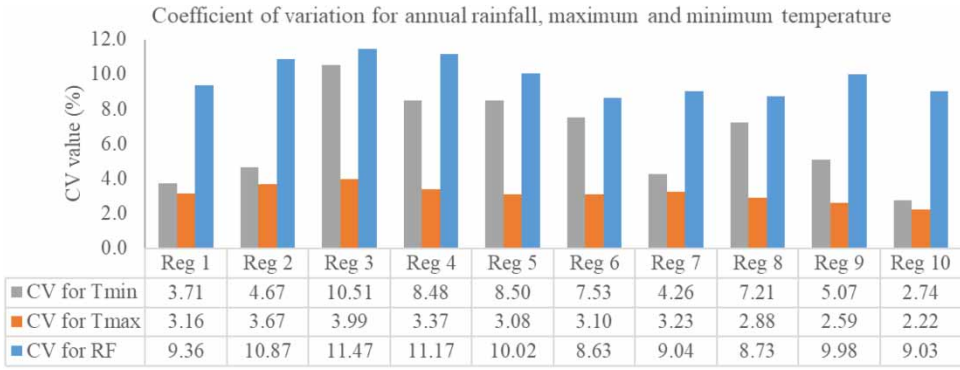

	Reg 1	Reg 2	Reg 3	Reg 4	Reg 5	Reg 6	Reg 7	Reg 8	Reg 9	Reg 10
CV for Tmin	3.71	4.67	10.51	8.48	8.50	7.53	4.26	7.21	5.07	2.74
CV for Tmax	3.16	3.67	3.99	3.37	3.08	3.10	3.23	2.88	2.59	2.22
CV for RF	9.36	10.87	11.47	11.17	10.02	8.63	9.04	8.73	9.98	9.03

Figure 3 | CV across the region in the study area.

(30.99% of the sub-basin) while in January (61.36%), June (15.3%), July (20.23%), and September (62.51%) of some regions show moderate rainfall variability ($20 < CV > 30$). In August, low variability of rainfall for all regions (100%) of the study area was observed as shown in Figure 2 and this result is more or less similar to the studies by Abera *et al.* (2020). The highest value of the CV was found in March in the northeast part (region 2) and the lowest was recorded in August in the southeast of the sub-basin (region 8). The study's findings regarding the significant variability in annual rainfall across different regions, particularly in the eastern part of the study area exhibiting the highest variability. Region 3 shows the highest coefficient of variability in annual rainfall followed by regions 2 and 4. It also emphasizes that this variability has had adverse effects on the rain-dependent population in terms of crop production, livestock, and overall livelihood. The adverse effects on crop production, livestock, and overall livelihood emphasize the importance of understanding and addressing the impact of this variability on vulnerable communities.

The study's results suggest that, overall, the maximum and minimum temperatures in the study area exhibit lower temporal variations compared to rainfall, as illustrated in Figures 4 and 5. While most regions show lower variability in terms of minimum and maximum annual and monthly temperatures ($CV < 20$), specific areas with a CV exceeding 30% indicate vulnerability to natural disasters such as floods and droughts (Haile 1988; Hare 2003). The average vulnerability of

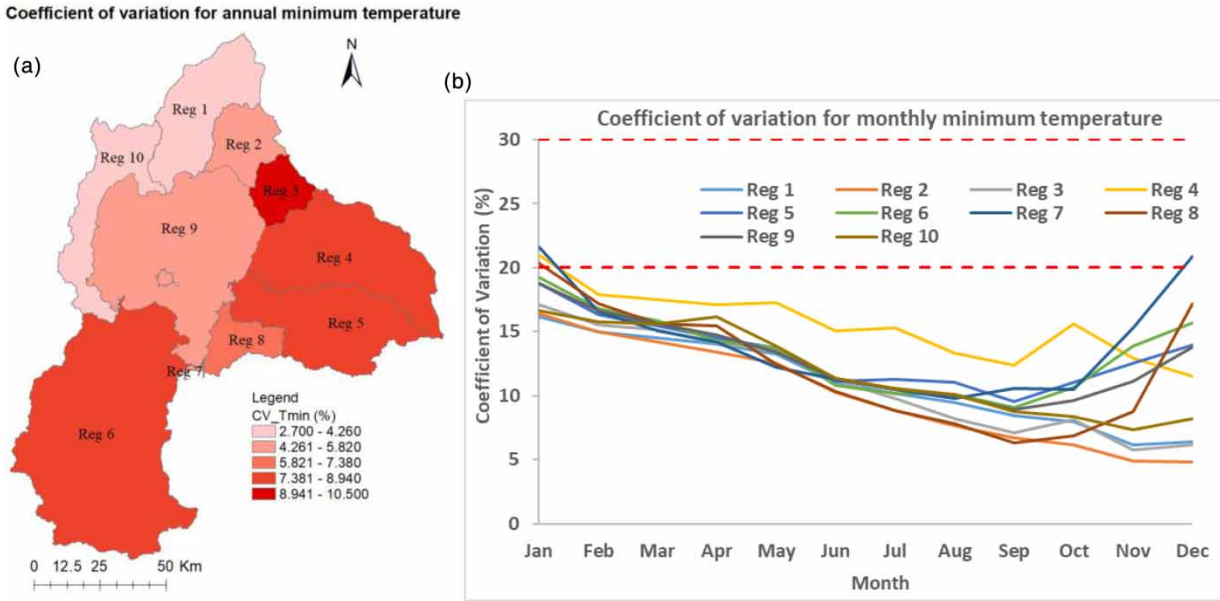

Figure 4 | CV for (a) annual and (b) monthly minimum temperature.

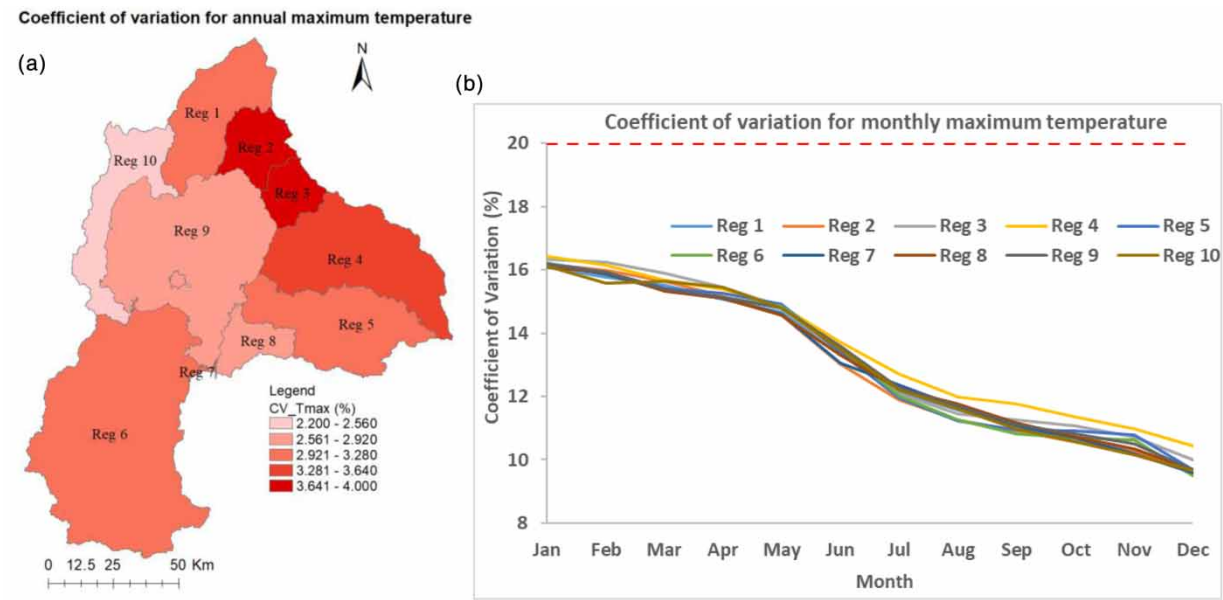

Figure 5 | CV for (a) annual and (b) monthly maximum temperature.

approximately 58.04% throughout the year underscores the potential impact of climate-related events on the study area. Understanding the vulnerability to natural disasters and the variability in temperature patterns can be crucial for developing appropriate adaptation and mitigation strategies. The highest CV for minimum temperature was observed in January in the Megech watershed (region 1), while the lowest was recorded in December in the northeast (region 2). For maximum temperature, the highest variation was found in January in the Rib watershed (region 4), with the lowest recorded in December in the Gumara watershed (region 5). The localized vulnerability to climate-related events highlighted in the study underscores the need for region-specific adaptation and mitigation measures (Yeshitila *et al.* 2019; Wubneh *et al.* 2023). Understanding the potential impact on different regions within the study area is crucial for developing targeted strategies to address the challenges posed by climate variability.

3.2. Trend analysis in climatic variables

The MK trend test and Sen's slope were applied to the study areas. The tests were applied in each month, annual mean, annual maximum, and annual minimum rainfall using a significance level of 5% and confidence level of 95% in each region (Verma *et al.* 2021). The obtained results are presented in Table 2. The annual rainfall in the study area was observed from 797.71 to 1,770.2 mm. The results indicate significant variations in annual rainfall across the Tana sub-basin, with the highest mean annual rainfall observed in region 6 with a value of 1,478.79 mm and the lowest mean value recorded in region 2 with a value of 985.83 mm. This heterogeneous distribution of rainfall suggests that there are significant variations in rainfall patterns within the sub-basin. Understanding these variations is crucial for assessing the potential impacts on water resources, agriculture, and ecosystems within the study area.

The MK trend test and Sen's slope were also applied to the study areas at each month, annual mean, annual maximum, and annual minimum for temperature data with a significance level of 5% and confidence level of 95% in each region. The obtained results are presented in Table 3. The annual minimum temperature in the study area ranges between 8.18 and 12.2 °C while the maximum temperature ranges between 24.00 and 29.95 °C. The results indicate significant variations in both annual minimum and maximum temperatures across the Tana sub-basin, with the highest annual maximum temperature observed in region 4 with a value of 29.95 °C and the lowest in region 6 with a value of 8.17 °C. This heterogeneous

Table 2 | Summary statistics for total annual rainfall

Annual rainfall

Regions	Obs.	Obs. with missing data	Obs. without missing data	Minimum	Maximum	Mean	Std. deviation
1	39	0	39	905.26	1,243.09	1,071.31	100.28
2	39	0	39	797.71	1,208.65	985.83	107.48
3	39	0	39	858.25	1,283.05	1,060.50	121.75
4	39	0	39	944.27	1,434.87	1,203.30	135.95
5	39	0	39	1,099.30	1,701.18	1,394.19	141.42
6	39	0	39	1,219.78	1,770.20	1,478.79	129.07
7	39	0	39	1,074.98	1,588.37	1,373.31	125.40
8	39	0	39	1,094.58	1,596.65	1,377.76	121.63
9	39	0	39	949.04	1,464.74	1,183.08	118.28
10	39	0	39	918.14	1,341.79	1,144.50	103.28

Table 3 | Summary statistics for minimum and maximum annual temperature

				Annual minimum temperature				Annual maximum temperature			
Regions	Obs.	Obs. with missing data	Obs. without missing data	Minimum	Maximum	Mean	Std. deviation	Minimum	Maximum	Mean	Std. deviation
1	36	0	36	11.59	14.42	13.48	0.68	25.54	28.63	27.45	0.73
2	36	0	36	11.66	13.44	12.75	0.47	24.08	27.12	25.93	0.82
3	36	0	36	12.03	14.86	13.42	0.63	25.08	28.69	27.03	0.99
4	36	0	36	9.65	15.34	12.79	1.34	25.75	29.95	27.94	1.12
5	36	0	36	8.18	11.88	10.52	0.89	24.02	27.55	25.96	0.88
6	36	0	36	8.17	12.04	10.55	0.90	24.00	27.20	25.93	0.80
7	36	0	36	9.02	13.36	10.80	0.81	24.15	27.81	25.95	0.80
8	36	0	36	11.11	13.15	12.08	0.52	25.24	28.69	27.41	0.89
9	36	0	36	9.76	13.45	12.27	0.89	25.48	28.75	27.54	0.79
10	36	0	36	12.20	15.62	14.54	0.80	25.15	28.22	27.02	0.70

distribution of temperature further emphasizes the significant variations in minimum temperature patterns within the sub-basin. Understanding these variations is crucial for assessing potential impacts on various sectors such as agriculture, water resource management, and public health.

Figures 6 and 7 represent the time series of annual rainfall and temperature in the sub-basin. The annual rainfall varied with location and ranged from a maximum of 1,770.2 mm recorded in 2017 in region 6 to a minimum of 797.71 mm in 1990 in region 2 during the period 1981–2020. The results of trend analysis, including the *p*-value from the MK test and the trend's slope (β) from Sen's estimator are presented in Table 4. The results of the MK test for annual rainfall data revealed

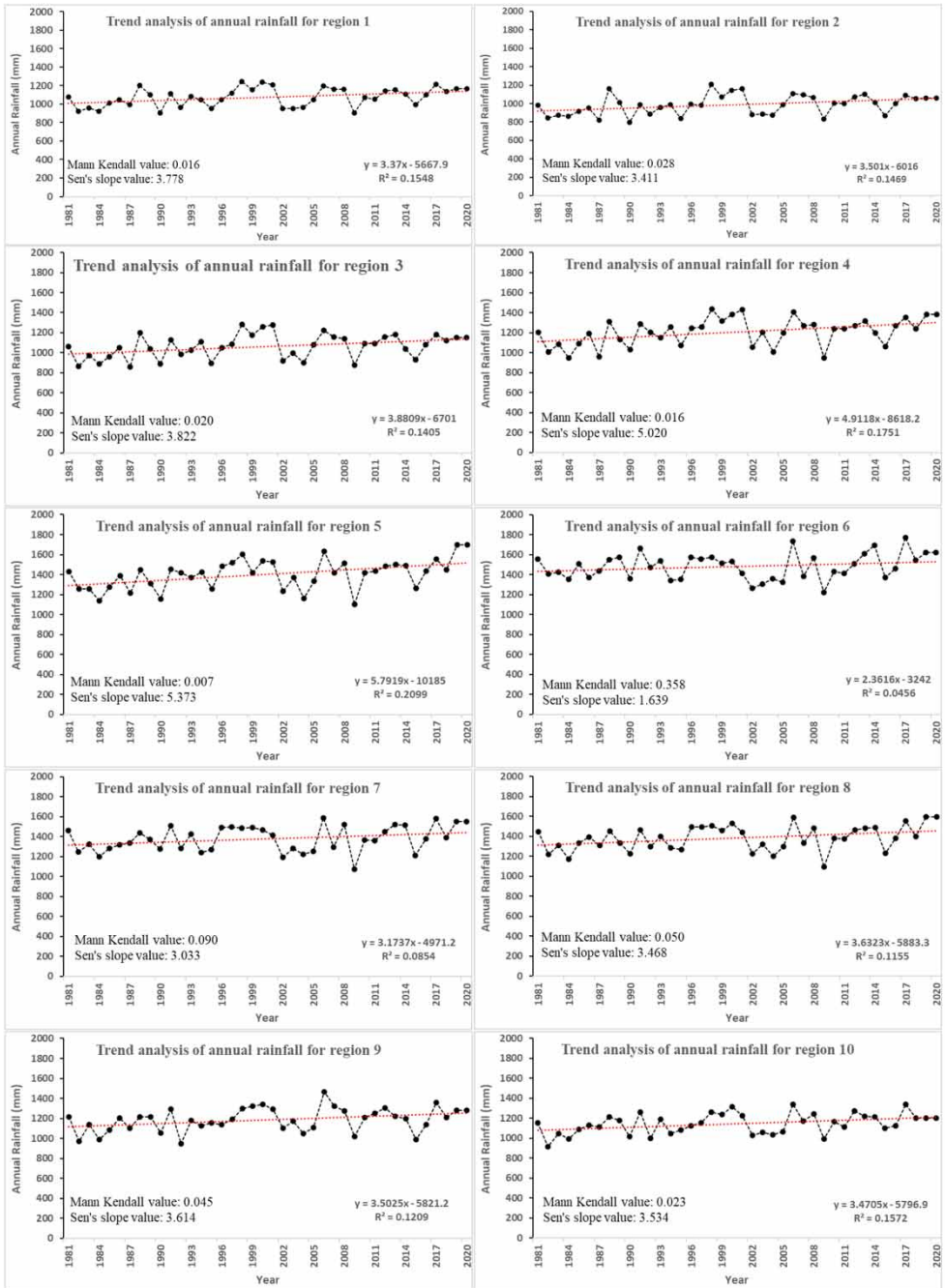

Figure 6 | Temporal and spatial annual rainfall trend and its significance level during 1981–2020.

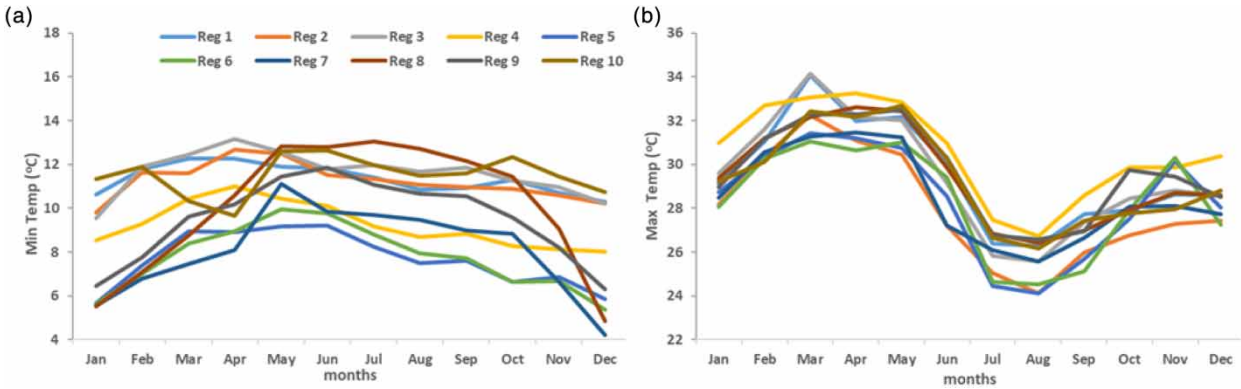

Figure 7 | Mean monthly (a) minimum temperature and (b) maximum temperature.

Table 4 | MK test results on annual time series rainfall with 5% significance

	MK test				Sen's nonparametric estimator of slope		
Regions	**Kendall's tau**	***S***	***P***	**Result**	**Sen's slope**	**Lower limit (95%)**	**Upper limit (95%)**
1	0.247	183	0.028	Trend	3.411	0.421	6.237
2	0.271	201	0.016	Trend	3.778	0.705	6.411
3	0.260	193	0.020	Trend	3.822	0.751	7.418
4	0.271	201	0.016	Trend	5.021	1.004	8.587
5	0.301	223	0.007	Trend	5.373	1.503	9.396
6	0.104	77	0.358	No trend	1.639	−1.868	5.935
7	0.190	141	0.090	No trend	3.033	−0.991	6.637
8	0.220	163	0.050	No trend	3.468	0.077	6.943
9	0.225	167	0.045	Trend	3.614	0.049	6.773
10	0.255	189	0.023	Trend	3.534	0.527	6.563

a statistically non-significant increasing trend at a 5% level of significance. A statistically non-significant increasing trend was observed for summer, spring, autumn, and winter rainfall at a 5% significance level for all regions while regions 2 and 3 in winter and region 6 in summer show a statistically non-significant decreasing trend. In region 1, annual rainfall varied from 905 mm in 1990 to 1,243 mm in 1998 with a non-significant increasing trend ($p > 0.05$). The areal annual rainfall in the study area shows a non-significant increment trend ($p > 0.05$) for all regions (Figure 6 and Table 4). The annual rainfall in region 2 ranged from 797.71 to 1,209 mm and a non-significant increasing trend ($p > 0.05$) was observed in the annual rainfall (Table 4). In different parts of Ethiopia, other studies also did not find a statistically significant trend in the annual rainfall (Viste *et al.* 2013; Mengistu *et al.* 2014). The MK test results and Sen's slope for annual rainfall across the regions are presented in Table 4. As depicted in the table, annual rainfall in the Tana sub-basin showed an increasing trend in most parts of the region. Only small sections in the southern and southeastern parts of the study area revealed no trend in annual rainfall.

The analysis of Sens slope indicates that annual rainfall has increased with a non-significant trend across all regions of the study area (Weldegerima *et al.* 2018). Specifically, non-significant increasing trends were observed for the months of May, September, and December in all regions, while the remaining months showed non-significant increasing and decreasing trends in different regions. The magnitude of the increasing range, as indicated by Sen's slope method, ranged from 1.639 to 5.373 mm/year (Table 4 and Figure 7). Most regions showed a Sen's slope/rainfall increment value ranging from 3 to 4 mm/year, with region 5 having the highest annual increment at 5.373 mm/year, region 4 at 5.021 mm/year, and region 6 at the lowest annual rainfall increment of 1.639 mm/year (Table 4). Overall, the study found a statistically non-significant increasing trend for all parts of the sub-basin, with temporal and regional variations in rainfall increments. The findings

are noted to be similar to studies conducted by Birara *et al.* (2020). It appears that the study indicates a general trend of non-significant increases in annual rainfall across the study area, with variations in the magnitude of the increase across different regions.

The results of the trend analysis, including the *p*-value from the MK test and the trend's slope (β) from Sen's estimator, are presented in Tables 5 and 6. The results of the MK test for annual minimum temperature data showed a statistically non-significant increasing trend in most regions, while regions 7, 8, and 10 showed no trend at a 5% level of significance. Similarly, a statistically non-significant increasing trend was observed for summer, spring, autumn, and winter minimum temperatures at a 5% significance level for all regions, with regions 7 and 8 in winter showing a statistically non-significant decreasing trend. The magnitude of the increasing range, as indicated by Sen's slope method, ranged from 0.001 to 0.080 °C/year (Table 5). All regions showed Sen's slope for minimum temperature increment, with region 4 having the highest annual increment and region 8 showing the lowest annual minimum temperature increment. The MK test results and Sen's slope for annual minimum temperature across the regions are presented in Table 5, indicating an increasing trend in annual minimum temperature in the Tana sub-basin.

The results of the trend analysis for annual maximum temperature data indicate a statistically non-significant increasing trend in all regions at a 5% level of significance. Similarly, a statistically non-significant increasing trend was observed for summer, spring, autumn, and winter maximum temperatures at a 5% significance level for all regions. The magnitude of

Table 5 | MK test results on annual time series minimum temperature with 5% significance

	MK test				Sen's nonparametric estimator of slope		
Regions	**Kendall's tau**	***S***	***P***	**Result**	**Sen's slope**	**Lower limit (95%)**	**Upper limit (95%)**
1	0.371	234	0.0015	Trend	0.034	0.015	0.050
2	0.429	270	0.0002	Trend	0.028	0.016	0.038
3	0.667	420	<0.0001	Trend	0.049	0.039	0.059
4	0.556	350	<0.0001	Trend	0.080	0.057	0.108
5	0.486	306	<0.0001	Trend	0.051	0.035	0.070
6	0.530	334	<0.0001	Trend	0.054	0.039	0.070
7	0.219	138	0.0620	No trend	0.018	−0.001	0.038
8	0.019	12	0.8809	No trend	0.001	−0.016	0.020
9	0.530	334	<0.0001	Trend	0.055	0.037	0.073
10	0.222	140	0.0583	No trend	0.027	−0.002	0.051

Table 6 | MK test results on annual time series maximum temperature with 5% significance

	MK test				Sen's nonparametric estimator of slope		
Regions	**Kendall's tau**	***S***	***P***	**Result**	**Sen's slope**	**Lower limit (95%)**	**Upper limit (95%)**
1	0.625	394	<0.0001	Trend	0.055	0.041	0.071
2	0.689	434	<0.0001	Trend	0.064	0.050	0.078
3	0.635	400	<0.0001	Trend	0.078	0.054	0.100
4	0.717	452	<0.0001	Trend	0.096	0.078	0.114
5	0.584	368	<0.0001	Trend	0.067	0.047	0.087
6	0.505	318	<0.0001	Trend	0.053	0.030	0.074
7	0.378	238	0.0012	Trend	0.043	0.020	0.064
8	0.683	430	<0.0001	Trend	0.069	0.055	0.088
9	0.562	354	<0.0001	Trend	0.054	0.034	0.071
10	0.495	312	<0.0001	Trend	0.048	0.028	0.067

the increasing range, as indicated by Sen's slope method, is from 0.043 to 0.096 °C/year (Table 6). All regions showed a Sen's slope for minimum temperature increment, with region 7 exhibiting the highest annual increment and region 4 (located in the eastern part of the study area) showing the lowest annual maximum temperature increment. The MK test results and Sen's slope for annual maximum temperature across the regions are presented in Table 6, indicating an increasing trend in annual maximum temperature in the Tana sub-basin.

Figure 7 shows the long-term trend in the minimum and maximum monthly temperature observed during the 1981–2016 periods. The temperatures ranged from 4.2 °C in December to 34.5 °C in March for the minimum and maximum temperature, respectively. These values are similar to those studied by Abera *et al.* (2020) for maximum temperature but the minimum temperature was recorded in February. The monthly average minimum and maximum varied from 7.66 to 11.61 °C and 28.01 to 30.56 °C, respectively.

According to the long-term average monthly temperature value, lower and higher values of monthly minimum temperature trends were observed in the Gumara watershed and Rib watershed, respectively. There was an increasing trend in Tmin and Tmax in all regions during the period 1981–2016, but it shows a non-significant trend. The increment in the magnitude of the temperature is supported in the study by Birara *et al.* (2020) but with a significant trend. The increment of the magnitude of temperature here is mainly related to deforestation and climate change which results from overcultivation and excessive pressure on natural resources (Anteneh 2022). The rise in temperature will lead to more evapotranspiration and is expected to increase the intensity of extreme weather events, change the amount and pattern of precipitation and impact the water resources of the study area. The variations in temperature and rainfall in the sub-basin affect agricultural activities, cropping patterns, society livelihoods and natural resources. As high population pressure and agricultural-dependent people of the study area, the rural livelihoods will be more severe since they are the direct victims of the society unless strategic measures should be taken. The vulnerability of rural households might be further aggravated if the variability of rainfall and temperature continues in the future and consequently results in drought, flood, and natural resources losses, appropriate adaptation strategies should be designed and implemented.

3.3. Rainfall seasonality

Figure 8 shows the distribution of SI value across the regions in the study area: Tana sub-basin. The value of the SI ranged between 0.87 and 1.03. The minimum SI values (0.87) were observed in region 6 in the southern part of the study area whereas the maximum values (1.03) were observed in region 3 in the northeastern part of the study area (Figure 9). The SI value increases from the southwest, southeast, south, and north to the east of the sub-basin (Figure 8). The amount of rainfall received and its seasonal distribution in the study area significantly affect its agricultural activity, natural vegetation and regional moisture (Mesfin *et al.* 2021; Wakjira *et al.* 2021). The SI is grouped into two categories in the study. Area of region one has mean SI values between 0.80 and 0.99 with marked seasonal with a long dry season which accounts for 36.69% of the total area, and region two has SI values from 1.0 to 1.19 with most rain in three or fewer months (63.31%) as shown in Table 1 and Figure 8. Most of the regions have ample amounts of rain but are concentrated in three or fewer months each year with considerable variability and trend (Weldegerima *et al.* 2018). Therefore, it is important to adjust the area's agricultural practices to the variability and trend of rainfall (Wakjira *et al.* 2021).

According to the rainfall variability and seasonality results in different regions, it is interesting to note that the highest CV in rainfall and the highest value of SI are observed in regions 3 and 4 in the eastern part of the study area. In addition, the study shows that the rainfall seasonality derived from mean PCI and the SI exhibit similar and direct graphical patterns in the study area. The regions with higher values of the SI are likely to experience rain for many months. Region 3 has the highest rainfall variability and SI, followed by region 4, while region 6 in the southern part of the study area has the lowest rainfall variability and SI. The results of the correlation between CV and SI across the regions are presented in Figure 9.

Figure 10 presents the distribution of the mean PCI of the annual rainfall of the Tana sub-basin across the regions from 1981 to 2020. As shown in the figure, uniform distribution of rainfall ($PCI < 10$) was not observed in the study area during the period 1981–2020. The value of PCI varied from 13.67 to 27.58. Minimum values of PCI were observed in region 9 at the center parts of the study area whereas the maximum values of PCI were observed in region 3 predominantly in the northeastern part of the study area.

According to the PCI value of the three classes (Oliver 1980; Belay *et al.* 2021; Edo *et al.* 2021), 57.5% of rainfall data in the sub-basin were shown a strong irregular precipitation distribution ($PCI > 20$) and closely similar to the ones studied by Dawit *et al.* (2019) while 41.5% were irregular precipitation concentration. The remaining 1% of PCI values represent

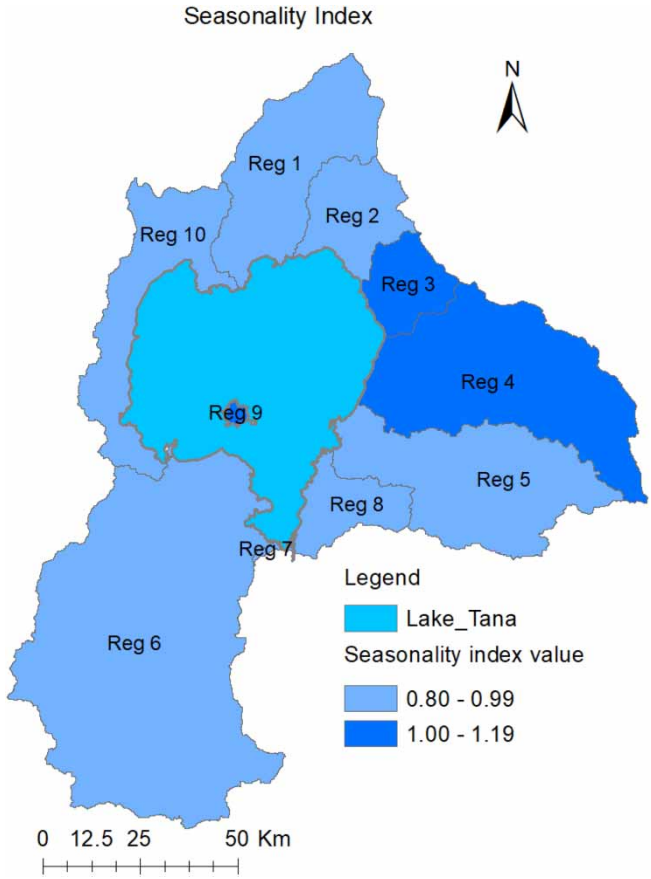

Figure 8 | SI value across the regions.

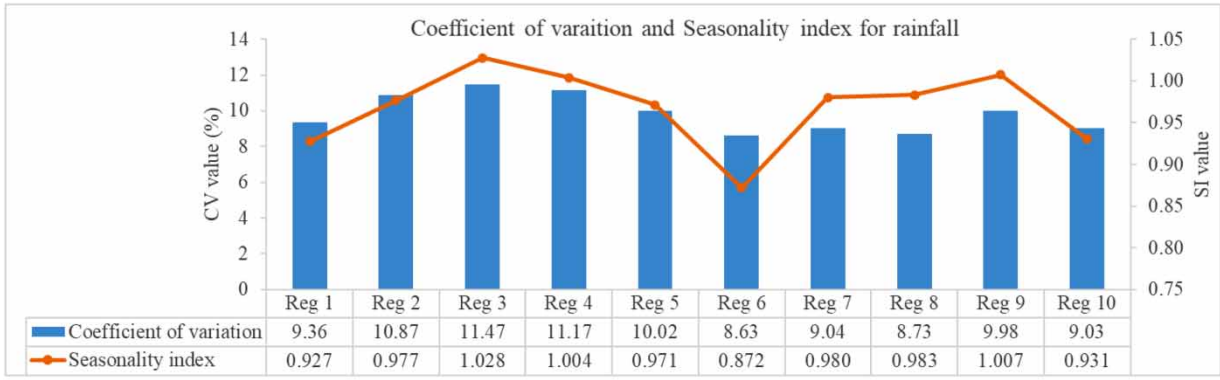

Figure 9 | Correlation of SI with CV for rainfall.

moderate precipitation concentration in the study area. According to the spatial and temporal distribution PCI, strong irregularity of annual, seasonal, and monthly precipitation distribution was observed. Irregularity of rainfall may lead to the occurrence of hydrological risks such as floods and drought (Yeshitila *et al.* 2019). In the years 1983, 1988, 1990, 2001, 2009, and 2010, hydrological risks such as flood occasions were indicated in the northeast parts of the sub-basin, and this may be the result of backflow experience from the Lake Tana to the downstream part in most of the rain season (Wubneh *et al.* 2023). The distribution of PCI values indicated that the distribution of rainfall in the study area was irregular spatially

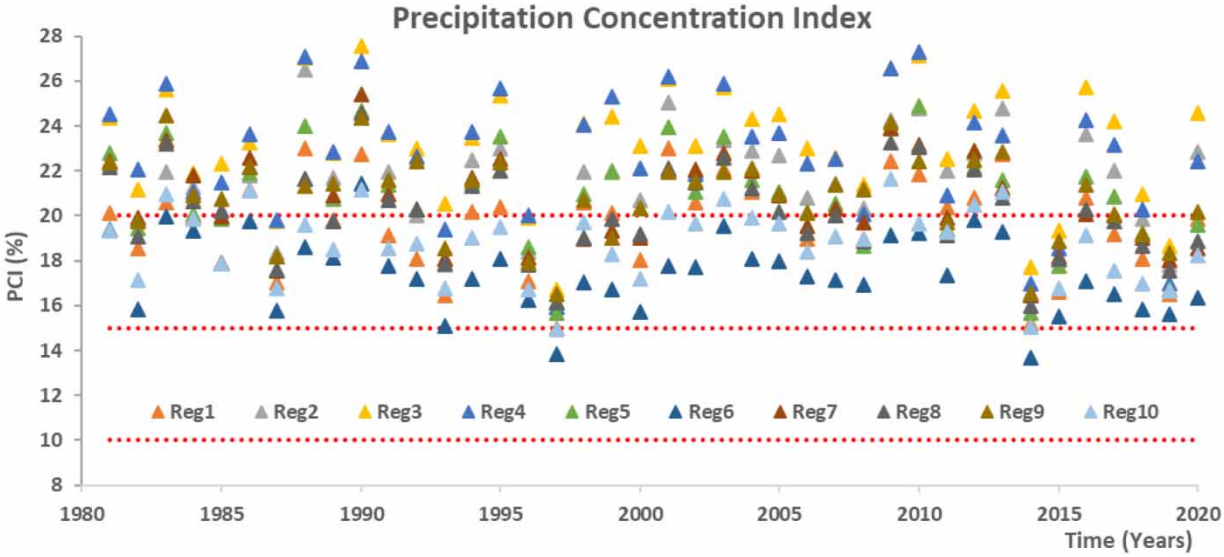

Figure 10 | PCI across the regions in the study area.

as well as temporally. Irregularity in the rainfall amount, intensity, onset, and offset days has a direct impact on agricultural activities, crop patterns, and livelihood. Spatially, the lowest PCI value difference (less than 2%) was observed in the year 1984 with a strong irregular rainfall occurrence. In the years 1985–1986, 1996–1997, 2014–2015, and 2019 PCI values also show small variation/range differences in all regions of the basin (Figure 10).

4. CONCLUSION

The study applied various statistical methods to analyze the variability and trend of climatic variables within the available rainfall and temperature data in the Tana sub-basin. The results indicated a statistically non-significant increasing trend in climatic variables across the study area. The precipitation distribution was found to be non-uniform, with a significant portion of rainfall exhibiting strong irregular distribution spatially and temporally. This irregularity in rainfall may lead to hydrological risks such as floods and drought. The study also concluded that the temporal variation of monthly rainfall is higher compared to the temporal variation of monthly temperature in the Tana sub-basin, implying that rainfall patterns are more variable and subject to change over time than temperature patterns. Given that the study area is predominantly dependent on rainfed agriculture, the variability and irregular distribution of rainfall may have significant implications for the livelihoods in the area. The study emphasizes the need for appropriate measures to mitigate and minimize the effects of climate variability on the livelihoods in the study area. The findings are expected to contribute valuable information for future similar studies.

ACKNOWLEDGEMENTS

The authors acknowledge the National Meteorology Agency (NMA) of Ethiopia for providing the observed data that were used in this study. The study was conducted on the Lake Tana sub-basin under the BRICS multilateral R&D project (BRICS2017-144) and NRF UID number 116021. The BRICS multilateral R&D project (BRICS2017-144) team is sincerely acknowledged. The authors also sincerely acknowledged Mr Sileshie Mesfin for the kind technical support and continuous follow-up that he made.

FUNDING SOURCES

The financial assistance of the South Africa National Research Foundation (NRF) is hereby acknowledged. The study is under the grant BRICS multilateral R&D project (BRICS2017-144), the NRF UID number 116021, and the Durban University of Technology UCDG Water Research Focus Area grant.

DATA AVAILABILITY STATEMENT

Data cannot be made publicly available; readers should contact the corresponding author for details.

CONFLICT OF INTEREST

The authors declare there is no conflict.

REFERENCES

Abera, A., Verhoest, N. E. C., Tilahun, S., Inyang, H. & Nyssen, J. 2020 Assessment of irrigation expansion and implications for water resources by using RS and GIS techniques in the Lake Tana Basin of Ethiopia. *Environmental Monitoring and Assessment* **193** (1), 13.

Abidoye, B. & Odusola, A. 2015 Climate change and economic growth in Africa: An econometric analysis. *Journal of African Economies* **24**, 1–25.

Addisu, S., Selassie, Y. G., Fissha, G. & Gedif, B. 2015 Time series trend analysis of temperature and rainfall in Lake Tana sub-basin, Ethiopia. *Environmental Systems Research* **4** (1), 25.

Alemu, M. L., Worqlul, A. W., Zimale, F. A., Tilahun, S. A. & Steenhuis, T. S. 2020 Water balance for a tropical lake in the volcanic highlands: Lake Tana, Ethiopia. *Water* **12** (10), 2737.

Allam, M. M., Jain Figueroa, A., McLaughlin, D. B. & Eltahir, E. A. 2016 Estimation of evaporation over the upper Blue Nile basin by combining observations from satellites and river flow gauges. *Water Resources Research* **52** (2), 644–659.

Anteneh, M. 2022 Climate variability patterns and farmers' perceptions of its impact on food production: A case study of the Gelda watershed in the Lake Tana Basin in Northwest Ethiopia. *Air, Soil and Water Research* **15**, 11786221221135093.

Asfaw, A., Simane, B., Hassen, A. & Bantider, A. 2018 Variability and time series trend analysis of rainfall and temperature in northcentral Ethiopia: A case study in Woleka sub-basin. *Weather and Climate Extremes* **19**, 29–41.

Awange, J. L., Forootan, E., Kuhn, M., Kusche, J. & Heck, B. 2014 Water storage changes and climate variability within the Nile Basin between 2002 and 2011. *Advances in Water Resources* **73**, 1–15.

Belay, A., Demissie, T., Recha, J. W., Oludhe, C., Osano, P. M., Olaka, L. A., Solomon, D. & Berhane, Z. 2021 Analysis of climate variability and trends in Southern Ethiopia. *Climate* **9** (6), 96.

Berihun, M. L., Tsunekawa, A., Haregeweyn, N., Meshesha, D. T., Adgo, E., Tsubo, M., Masunaga, T., Fenta, A. A., Sultan, D., Yibeltal, M. & Ebabu, K. 2019 Hydrological responses to land use/land cover change and climate variability in contrasting agro-ecological environments of the Upper Blue Nile basin, Ethiopia. *Science of The Total Environment* **689**, 347–365.

Birara, H., Pandey, R. P. & Mishra, S. K. 2018 Trend and variability analysis of rainfall and temperature in the Tana basin region, Ethiopia. *Journal of Water and Climate Change* **9** (3), 555–569.

Birara, H., Pandey, R. P. & Mishra, S. K. 2020 Projections of future rainfall and temperature using statistical downscaling techniques in Tana Basin, Ethiopia. *Sustainable Water Resources Management* **6** (5), 77.

Birsan, M.-V., Molnar, P., Burlando, P. & Pfaundler, M. 2005 Streamflow trends in Switzerland. *Journal of Hydrology* **314**, 312–329.

Clarke, C. L., Shackleton, S. E. & Powell, M. 2012 Climate change perceptions, drought responses and views on carbon farming amongst commercial livestock and game farmers in the semiarid Great Fish River Valley, Eastern Cape province, South Africa. *African Journal of Range & Forage Science* **29** (1), 13–23.

Dawit, M., Halefom, A., Teshome, A., Sisay, E., Shewayirga, B. & Dananto, M. 2019 Changes and variability of precipitation and temperature in the Guna Tana watershed, Upper Blue Nile Basin, Ethiopia. *Modeling Earth Systems and Environment* **5** (4), 1395–1404.

De Luís, M., Raventós, J., González-Hidalgo, J. C., Sánchez, J. R. & Cortina, J. 2000 Spatial analysis of rainfall trends in the region of Valencia (east Spain). *International Journal of Climatology* **20** (12), 1451–1469.

Dinku, T., Thomson, M., Cousin, R., del Corral, J., Ceccato, P., Hansen, J. & Connor, S. 2017 Enhancing National Climate Services (ENACTS) for development in Africa. *Climate and Development* **10** (7), 664–672.

Edo, A., Jilo, N. & Muluneh, F. 2021 Spatial-temporal rainfall trend and variability assessment in the Upper Wabe Shebelle River Basin, Ethiopia: Application of innovative trend analysis method. *Journal of Hydrology: Regional Studies* **37**, 100915.

Enyew, B. 2014 Assessment of the impact of climate change on hydrological drought in Lake Tana Catchment, Blue Nile Basin, Ethiopia. *Journal of Geology & Geosciences* **03**, 1–17.

Esayas, B., Simane, B., Teferi, E., Ongoma, V. & Tefera, N. 2019 Climate variability and farmers' perception in Southern Ethiopia. *Advances in Meteorology* **2019**, 7341465.

Eshetu, Z., Simane, B., Tebeje, G., Negatu, W., Amsalu, A., Berhanu, A., Bird, N., Welham, B. & Trujillo, N. C. 2014 *Climate Finance in Ethiopia*. Overseas Development Institute, London and Climate Science Centre, Addis Ababa.

Field, C. B. 2014 *Climate Change 2014–Impacts, Adaptation and Vulnerability: Regional Aspects*. Cambridge University Press, Cambridge, UK.

Getachew, B. & Manjunatha, B. R. 2021 Climate change projections and trends simulated from the CMIP5 models for the Lake Tana sub-basin, the Upper Blue Nile (Abay) River Basin, Ethiopia. *Environmental Challenges* **5**, 100385.

Gissila, T., Black, E., Grimes, D. I. F. & Slingo, J. M. 2004 Seasonal forecasting of the Ethiopian summer rains. *International Journal of Climatology* **24**, 1345–1358.

Gocic, M. & Trajkovic, S. 2013 Analysis of changes in meteorological variables using Mann-Kendall and Sen's slope estimator statistical tests in Serbia. *Global and Planetary Change* **100**, 172–182.

Habte, A., Mamo, G., Worku, W., Ayalew, D. & Gayler, S. 2021 Spatial variability and temporal trends of climate change in southwest Ethiopia: Association with farmers' perception and their adaptation strategies. *Advances in Meteorology* **2021**, 3863530.

Haile, T. 1988 Causes and characteristics of drought in Ethiopia. *Ethiopian Journal of Agricultural Sciences* **10**, 85–97.

Haile, A. T., Rientjes, T., Gieske, A. & Gebremichael, M. 2009 Rainfall variability over mountainous and adjacent lake areas: The case of lake Tana Basin at the source of the Blue Nile River. *Journal of Applied Meteorology and Climatology* **48** (8), 1696–1717.

Hare, B. 2003 *Assessment of Knowledge on Impacts of Climate Change – Contribution to the Specification of Art. 2 of the UNFCCC: Impacts on Ecosystems, Food Production, Water and Socio-economic Systems*. WBGU, Berlin, Article ID 60–62.

Hassan, Z., Shamsudin, S. & Harun, S. 2014 Application of SDSM and LARS-WG for simulating and downscaling of rainfall and temperature. *Theoretical and Applied Climatology* **116** (1), 243–257.

IPCC 2012 Managing the risks of extreme events and disasters to advance climate change adaptation. In: *A Special Report of Working Groups I and II of the Intergovernmental Panel on Climate Change* (Field, C. B., Barros, V., Stocker, T. F., Qin, D., Dokken, D. J., Ebi, K. L., Mastrandrea, M. D., Mach, K. J., Plattner, G.-K., Allen, S. K., Tignor, M. & Midgley, P. M., eds). Cambridge University Press, Cambridge, UK, p. 582.

IPCC 2013 *Climate Change 2013: The Physical Science Basic Contribution of Working Group I to the Fifth Assessment Report of the Intergovernmental Panel on Climate Change*. Cambridge University Press, Cambridge, UK.

Kassie, B. T., Rötter, R. P., Hengsdijk, H., Asseng, S., Van Ittersum, M. K., Kahiluoto, H. & Van Keulen, H. 2014 Climate variability and change in the Central Rift Valley of Ethiopia: Challenges for rainfed crop production. *The Journal of Agricultural Science* **152** (1), 58–74.

Kebede, S., Travi, Y., Alemayehu, T. & Marc, V. 2006 Water balance of Lake Tana and its sensitivity to fluctuations in rainfall, Blue Nile basin, Ethiopia. *Journal of Hydrology* **316** (1), 233–247.

Keller, M. 2009 *Climate Risks and Development Projects. Assessment Report for a Community-Level Project in Gudru, Oromyia, Ethiopia.* Bread for All, Bern. https://citeseerx.ist.psu.edu/document?repid=rep1&type=pdf&doi=44048c741fbd2f98e40623b787c76e2ffcccdb0d.

Kendall, M. G. 1975 *Rank Correlation Methods*. Griffin, London.

Kim, U. & Kaluarachchi, J. 2009 Climate change impacts on water resources in the Upper Blue Nile River Basin, Ethiopia. *JAWRA Journal of the American Water Resources Association* **45**, 1361–1378.

Korecha, D. & Barnston, A. G. 2007 Predictability of June September rainfall in Ethiopia. *Monthly Weather Review* **135**, 628.

Krishan, G., Garg, S., Krishan, P., Gopal, A., Someshwar Rao, M., Kumar, R. & Aggarwal, R. 2012 *Rainfall Trend Analysis in Saharanpur District of Uttar Pradesh-Agricultural Context*.

Kumar, K., Verma, S., Sahu, R. & Verma, M. 2023 Analysis of rainfall trends in India, incorporating non-parametric tests and wavelet synopsis over the last 117 years. *Journal of Environmental Informatics Letters* **10**, 74–88.

Makenzi, P., Ketiem, P., Omondi, P., Maranga, E. & Wekesa, C. 2013 Trend analysis of climate change and its impacts on crop productivity in the Lower Tana River Basin, Kenya. *Octa Journal of Environmental Research* **1**, 237–248.

Mann, H. B. 1945 Nonparametric tests against trend. *Econometrica* **13** (3), 245–259.

McSweeney, C., New, M. & Lizcano, G. 2008 'UNDP climate change Country profiles Ethiopia,' 2008. Available from: http://country-profiles.geog.ox.ac.uk. (accessed 2 August 2023).

Mengistu, D., Bewket, W. & Lal, R. 2014 Recent spatiotemporal temperature and rainfall variability and trends over the Upper Blue Nile River Basin, Ethiopia. *International Journal of Climatology* **34** (7), 2278–2292.

Mesfin, S., Adem, A. A., Mullu, A., Melesse, A. M., 2021 Historical trend analysis of rainfall in Amhara national regional state. In: *Nile and Grand Ethiopian Renaissance Dam: Past, Present and Future* (Melesse, A. M., Abtew, W. & Moges, S. A., eds). Springer International Publishing, Cham, pp. 475–491. https://doi.org/10.1007/978-3-030-76437-1_25.

Meshesha, T., Khare, D. & Tripathi, S. 2018 Spatiotemporal trend analysis of rainfall and temperature, and its implication on crop production. *Journal of Water and Climate Change* **10**, jwc2018064.

NMSA 1996 *Climatic and Agro-Climatic Resources of Ethiopia*. NMSA Meteorological Research Report Series. Vol. 1. National Meteorological Service Agency, Addis Ababa, No. 1, 137 p.

Oliver, J. E. 1980 Monthly precipitation distribution: A comparative index. *The Professional Geographer* **32** (3), 300–309.

Omondi, P. A. o., Awange, J. L., Forootan, E., Ogallo, L. A., Barakiza, R., Girmaw, G. B., Fesseha, I., Kululetera, V., Kilembe, C., Mbati, M. M., Kilavi, M., King'uyu, S. M., Omeny, P. A., Njogu, A., Badr, E. M., Musa, T. A., Muchiri, P., Bamanya, D. & Komutunga, E. 2014 Changes in temperature and precipitation extremes over the Greater Horn of Africa region from 1961 to 2010. *International Journal of Climatology* **34** (4), 1262–1277.

Reidmiller, D. A. C., Easterling, D., Kunkel, K., Lewis, K., Maycock, T. & Stewart, B. 2018 *Fourth National Climate Assessment, Impacts, Risks, and Adaptation in the United States*, Vol. 2. US Global Change Research Program, Washington, DC.

Saroar, M. M. & Filho, W. L. 2016 Adaptation through climate smart agriculture: Status and determinants in coastal Bangladesh. In: *Climate Change Adaptation, Resilience and Hazards* (Leal Filho, W., Musa, H., Cavan, G., O'Hare, P. & Seixas, J., eds.). Springer, Cham, pp. 157–178.

Segele, Z. T. & Lamb, P. J. 2005 Characterization and variability of Kiremt rainy season over Ethiopia. *Meteorology and Atmospheric Physics* **89**, 153–180.

Seleshi, Y. & Zanke, U. 2004 Recent changes in rainfall and rainy days in Ethiopia. *International Journal of Climatology* **24**, 973–983.

Sen, P. K. 1968 Estimates of the regression coefficient based on Kendall's Tau. *Journal of the American Statistical Association* **63** (324), 1379–1389.

Setegn, S. G., Srinivasan, R. & Dargahi, B. 2008 Hydrological modeling in the Lake Tana basin, Ethiopia using SWAT model. *The Open Hydrology Journal* **2**, 49–62.

Setegn, S., Srinivasan, R., Melesse, A. & Dargahi, B. 2009 SWAT model application and prediction uncertainty analysis in the Lake Tana Basin, Ethiopia. *Hydrological Processes* **24**, 357–367.

Tenagashaw, D. Y. & Andualem, T. G. 2022 Analysis and characterization of hydrological drought under future climate change using the SWAT model in Tana sub-basin, Ethiopia. *Water Conservation Science and Engineering* **7** (2), 131–142.

Tesfaw, B. A., Dzwairo, B. & Sahlu, D. 2023 Assessments of the impacts of land use/land cover change on water resources: Tana Sub-Basin, Ethiopia. *Journal of Water and Climate Change* **14** (2), 421–441.

UNFCCC 2007 *United Nations Framework Convention on Climate Change: Climate Change: Impacts, Vulnerabilities and Adaptation in Developing Countries*. Climate Change Secretariat, Bonn, pp. 471–474.

Verma, S., Prasad, A. D., Verma, M. K., 2021 Trend analysis and rainfall variability of monthly rainfall in Sheonath River Basin, Chhattisgarh. In: *Proceedings of Recent Trends in Civil Engineering* (Pathak, K. K., Bandara, J. M. S. J. & Agrawal, R., eds). Springer Singapore, Singapore, pp. 777–790.

Verma, S., Prasad, A. D., Verma, M. K., 2022 Trends of rainfall and temperature over Chhattisgarh during 1901–2010. In: *Proceedings of Advanced Modelling and Innovations in Water Resources Engineering* (Rao, C. M., Patra, K. C., Jhajharia, D. & Kumari, S., eds). Springer Singapore, Singapore, pp. 3–19.

Viste, E., Korecha, D. & Sorteberg, A. 2013 Recent drought and precipitation tendencies in Ethiopia. *Theoretical and Applied Climatology* **112** (3), 535–551.

Wakjira, M., Peleg, N., Anghileri, D., Molnar, D., Alamirew, T., Six, J. & Molnar, P. 2021 Rainfall seasonality and timing: Implications for cereal crop production in Ethiopia. *Agricultural and Forest Meteorology* **310**, 108633.

Walsh, R. & Lawler, D. 1981 Rainfall seasonality: Description, spatial patterns and change through time. *Weather* **36** (7), 201–208.

Weldegerima, T. M., Zeleke, T. T., Birhanu, B. S., Zaitchik, B. F. & Fetene, Z. A. 2018 Analysis of rainfall trends and its relationship with SST signals in the Lake Tana Basin, Ethiopia. *Advances in Meteorology* **2018**, 5869010.

Worku, T., Khare, D. & Tripathi, S. K. 2018 Spatiotemporal trend analysis of rainfall and temperature, and its implication on crop production. *Journal of Water and Climate Change* **10** (4), 799–817. Article ID.

Wubneh, M. A., Alemu, M. G., Fekadie, F. T., Worku, T. A., Demamu, M. T. & Aman, T. F. 2023 Meteorological and hydrological drought monitoring and trend analysis for selected gauged watersheds in the Lake Tana basin, Ethiopia: Under future climate change impact scenario. *Scientific African* **20**, e01738.

Yeshitila, T., Moges, M. A., Dessalegn, T. A., Melesse, A. M., 2019 Chapter 32 – Climate-induced flood inundation in Fogera-Dera Floodplain, Lake Tana basin, Ethiopia. In: *Extreme Hydrology and Climate Variability* (Melesse, A. M., Abtew, W. & Senay, G., eds). Elsevier, pp. 407–418. Available from: https://www.sciencedirect.com/science/article/pii/B9780128159989000324?via%3Dihub.

First received 25 September 2023; accepted in revised form 16 February 2024. Available online 29 February 2024